



Analytical formulas for penetration of a long rigid projectile including the effect of cavitation

M.B. Rubin

Faculty of Mechanical Engineering, Technion – Israel Institute of Technology, 32000 Haifa, Israel

ARTICLE INFO

Article history:

Received 30 December 2010
Received in revised form
13 September 2011
Accepted 26 September 2011
Available online 10 October 2011

Keywords:

Cavitation
Drag force
Elastic-plastic
Penetration mechanics
Ovoid of Rankine

ABSTRACT

Analytical expressions for penetration of a long rigid projectile with a nose shape of an ovoid of Rankine into a semi-infinite incompressible elastic–perfectly-plastic target have been developed earlier. Using these expressions it is shown that the drag force applied by the target on the projectile can be approximated as a bilinear function of the square of the penetration velocity in terms of three non-dimensional constants $\{\Sigma_c, \alpha_c, \beta_{\max}\}$. The value of Σ_c characterizes the constant value of the drag force for low penetration velocities. Cavitation (separation of the target material from the projectile's surface) first occurs when the penetration velocity reaches a value associated with α_c . The parameter β_{\max} controls the dependence of the drag force on the square of the penetration velocity as the separation point on the projectile's surface approaches its tip. Analytical expressions for these constants are determined in terms of the material parameters of the target material. Also, a simple formula for the penetration depth is developed and a method is proposed for determining the constants $\{\Sigma_c, \alpha_c, \beta_{\max}\}$ directly from experimental data.

© 2011 Elsevier Ltd. All rights reserved.

1. Introduction

Backman and Goldsmith [3] document scientific interest in penetration mechanics from the beginning of the 19th century and a collection of experimental data can be found in [2]. Here, attention is limited to the case of a rigid projectile penetrating a semi-infinite incompressible elastic–perfectly-plastic target. Fig. 1 shows a typical axisymmetric projectile which has a nose that smoothly transitions to a circular cylinder of radius R . The projectile moves with velocity V in the negative \mathbf{e}_3 direction without rotation so the balance of linear momentum for the motion is given by

$$M\dot{V} = -F, \quad (1)$$

where M is the projectile's mass and F is the drag force applied in the positive \mathbf{e}_3 direction by the target material on the projectile. Letting s be the instantaneous depth of penetration and using the specifications

$$V = \dot{s}, \quad V(0) = V_0, \quad s(0) = 0, \quad (2)$$

it is convenient to introduce the normalized variables

$$\Sigma = \frac{F}{\pi R^2 Y}, \quad \alpha = \frac{\rho V^2}{Y}, \quad \alpha_0 = \frac{\rho V_0^2}{Y}, \quad \lambda = \frac{2\rho\pi R^2 s}{M}. \quad (3)$$

Then, multiplying Eq. (1) by V yields

$$\dot{\alpha} = -\Sigma\dot{\lambda}, \quad \frac{d\alpha}{d\lambda} = -\Sigma. \quad (4)$$

In these expressions, V_0 is the impact velocity, and $\{\rho, Y\}$ are, respectively, the constant density and yield strength (in uniaxial stress) of the target. Moreover, Σ is the normalized drag force that the target applies to the projectile, α is a normalized inertia (kinetic energy) in the target and λ is the normalized instantaneous depth of penetration.

Hill [6] describes research done between May 1943 and March 1946 on cavitation during penetration of a rigid projectile into metal. He notes that due to melting at the projectile's surface the effects of friction are negligible. Consequently the traction vector \mathbf{t} applied by the target material on the projectile can be approximated as a contact pressure P applied in the opposite direction to the outward unit normal \mathbf{n} to the projectile's surface (see Fig. 1)

$$\mathbf{t} = -P\mathbf{n}. \quad (5)$$

E-mail address: mbrubin@tx.technion.ac.il.

predicted by Eq. (19) appears to be a nonlinear function of α during cavitation. However, the numerical simulations of Batra and Wright [4] and of Rosenberg and Dekel [9] indicate the unexpected result that the drag force during cavitation is nearly linear in α . Specifically, Rosenberg and Dekel [9] proposed an expression for the drag force Σ for the full range of penetration velocities, which can be rewritten in the form

$$\Sigma = \Sigma_{\text{RD}} = \Sigma_{\text{cRD}} + \beta_{\text{RD}}(\alpha - \alpha_{\text{cRD}}), \quad \Sigma_{\text{cRD}} = B\alpha_{\text{cRD}},$$

$$\alpha_{\text{cRD}} = \frac{\rho V_{\text{cRD}}}{Y}, \quad \beta_{\text{RD}} = \frac{B}{2}, \quad (21)$$

where Σ_{cRD} characterizes the low velocity drag force, α_{cRD} characterizes the normalized velocity at the onset of cavitation, B is a positive constant that characterizes the shape of the projectile's nose and the Macaulay brackets $\langle x \rangle$ are defined by

$$\langle x \rangle = \frac{1}{2}(x + |x|). \quad (22)$$

Although the drag force in Eq. (21) is characterized by three constants $\{\Sigma_{\text{cRD}}, \alpha_{\text{cRD}}, \beta_{\text{RD}}\}$ Rosenberg and Dekel [9] made an assumption that effectively reduced the number of constants to two $\{\alpha_{\text{cRD}}, \beta_{\text{RD}}\}$. It should be emphasized that the empirical values of these constants were obtained in [9] by calibration with numerical simulations for different targets and different projectile noses. Moreover, Rosenberg and Dekel [9] developed an expression for the penetration depth of a projectile with impact velocity V_0 which can be rewritten in the form

$$\lambda_{\text{IRD}} = \frac{1}{\Sigma_{\text{cRD}}} \left[(\alpha_0 - \langle \alpha_0 - \alpha_{\text{cRD}} \rangle) + \frac{\Sigma_{\text{cRD}}}{\beta_{\text{RD}}} \ln \left(1 + \frac{\langle \alpha_0 - \alpha_{\text{cRD}} \rangle}{2\alpha_{\text{cRD}}} \right) \right], \quad (23)$$

where use has been made of the normalized variables (3) and (21). In particular, it was demonstrated that this functional form can be used to predict accurate values of the penetration depth for a range of targets, nose shapes and impact velocities. Moreover, Rosenberg and Dekel [9] showed that the value of α_{cRD} depends on both the geometry of the projectile's nose and on the material properties of the target, whereas $\beta_{\text{RD}} = B/2$ is an empirical constant that depends only on the geometry of the nose of the projectile. Specifically, Rosenberg and Dekel [9] found that values of B for flat, spherical, conical and ogival noses are given by

$$B = 1.25 \text{ (flat)}, \quad B = 0.5 \text{ (spherical)}, \quad B = 0.24 \text{ (conical)},$$

$$B = 0.15 \text{ (ogival)}. \quad (24)$$

In this regard, it is unclear why the simulations of Batra and Wright [4] for a spherical nosed projectile suggest that for $(2 \leq \alpha \leq 6)$ the value of B controlling the slope of the Σ - α curve is given by $0.01546 (=2 \times 0.0773)$ instead of the value 0.5 in Eq. (24).

The objective of this paper is to provide theoretical support for conclusions of the type (21) and (23) which indicate that below a critical value V_c of the penetration velocity V ($\alpha < \alpha_c$) the drag force is nearly constant and above the critical value V_c ($\alpha \geq \alpha_c$) the drag force can be approximated as a linear function of α . This is accomplished by using the simplified expressions in [8], which are based on the full analysis in [12] for flow past an ovoid of Rankine. In particular, it will be shown that an accurate approximation of Σ for this theory is given by

$$\Sigma = \Sigma_{\text{simple}} = \Sigma_c + \beta_{\text{max}}(\alpha - \alpha_c), \quad (25)$$

and that the final value λ_f of the normalized penetration depth is obtained by substituting Eq. (25) into Eq. (4) and integrating the

result using the initial conditions (3) and the final condition that α vanishes to obtain the expression

$$\lambda_f = \frac{1}{\Sigma_c} \left[(\alpha_0 - \langle \alpha_0 - \alpha_c \rangle) + \frac{\Sigma_c}{\beta_{\text{max}}} \ln \left(1 + \frac{\beta_{\text{max}} \langle \alpha_0 - \alpha_c \rangle}{\Sigma_c} \right) \right]. \quad (26)$$

Expressions (25) and (26) are similar to Eqs. (21) and (23) except that they depend on three constants $\{\Sigma_c, \alpha_c, \beta_{\text{max}}\}$ instead of only the two constants $\{\alpha_{\text{cRD}}, \beta_{\text{RD}}\}$ in Eqs. (21) and (23). Moreover, in Section 2 analytical expressions for the constants $\{\Sigma_c, \alpha_c, \beta_{\text{max}}\}$ are developed that depend on the value G/Y of the target material and on the maximum value α_{max} of α for the range of impact velocities of consideration

$$\Sigma_c = \Sigma_c \left(\frac{G}{Y} \right), \quad \alpha_c = \alpha_c \left(\frac{G}{Y} \right), \quad \beta_{\text{max}} = \beta_{\text{max}} \left(\frac{G}{Y}, \alpha_{\text{max}} \right). \quad (27)$$

Also, it is noted that the result (26) differs from the well known Poncelet solution [3], which depends on two empirical constants and does not include the fact that the drag force is nearly constant for $\alpha < \alpha_c$. In this regard, the Poncelet equation can be considered applicable when the velocity dependent part of the drag force due to cavitation dominates the constant low velocity value of drag associated plasticity in the target.

An outline of this paper is as follows. Section 2 reviews some aspects of the solution developed in [12] and records simplified expressions given in [8]. Also, analytical expressions are given for the three constants (27). Section 3 discussed specific examples and Section 4 presents conclusions and discussion.

2. Basic equations for an ovoid of Rankine

The velocity field \mathbf{v} in the target around an ovoid of Rankine is a special case of flow of an incompressible fluid with a velocity potential ϕ for which

$$\mathbf{v} = \nabla \phi, \quad \nabla^2 \phi = 0. \quad (28)$$

Also, the Cauchy stress \mathbf{T} is expressed in the form

$$\mathbf{T} = -p\mathbf{I} + \mathbf{T}', \quad \mathbf{T}' \cdot \mathbf{I} = 0, \quad (29)$$

where the pressure p is an arbitrary function of position \mathbf{x} and time t , \mathbf{T}' is the deviatoric part of \mathbf{T} and $\mathbf{A} \cdot \mathbf{B} = \text{tr}(\mathbf{AB}^T)$ is the inner product between two second order tensors $\{\mathbf{A}, \mathbf{B}\}$. It then follows that in the absence of body force the balance of linear momentum can be written in the form

$$\nabla \left[\rho \left(\frac{\partial \phi}{\partial t} + \frac{1}{2} \mathbf{v} \cdot \mathbf{v} \right) + p \right] = \text{div } \mathbf{T}'. \quad (30)$$

Following the work in [12] the shape of an ovoid of Rankine is given by

$$r = \hat{r}(\xi) = \left[\frac{R^2 - \xi^2}{2} + \frac{\xi}{2} (\xi^2 + 2R^2)^{1/2} \right]^{1/2}, \quad (31)$$

where the variable ξ is defined by Eq. (11). Moreover, the velocity potential ϕ can be expressed in terms of the potentials of a moving point source and a uniform stream to obtain

$$\phi = \frac{\dot{z}_3 R^2}{4(\xi^2 + r^2)^{1/2}}. \quad (32)$$

It then can be shown that the rate of deformation tensor \mathbf{D} associated with the velocity gradient \mathbf{L} is a deviatoric tensor \mathbf{D}' , such that

$$\mathbf{L} = \partial \mathbf{v} / \partial \mathbf{x}, \quad \mathbf{D} = \frac{1}{2}(\mathbf{L} + \mathbf{L}^T), \quad \mathbf{D}' = \mathbf{D}, \quad \mathbf{D}' \cdot \mathbf{I} = 0. \quad (33)$$

In particular, this velocity field provides a realistic model for penetration problems since it ensures impenetrability of the target material with the surface of the nose of the projectile with the ovoid shape (see Fig. 2). This velocity field has also been used by Alekseevskii [1] and Tate [10,11] to study penetration problems.

In the solution presented in [12] the strains in the elastic region of the target are assumed to be small and the deviatoric stress in that region is determined by the equations

$$\mathbf{T}' = 2G\boldsymbol{\epsilon}', \quad \frac{\partial \boldsymbol{\epsilon}'}{\partial t} = \mathbf{D}', \quad \text{div } \mathbf{T}' = 0. \quad (34)$$

In the plastic region the strains can be arbitrarily large and \mathbf{T}' is specified by the Levy-Mises equation

$$\mathbf{T}' = Y\sqrt{\frac{2}{3}} \frac{\mathbf{D}'}{|\mathbf{D}'|}. \quad (35)$$

In particular, it was shown in [12] that for an ovoid of Rankine (35) yields the special result that the divergence of \mathbf{T}' can be expressed as the gradient of a scalar

$$\text{div } \mathbf{T}' = \nabla \left[-Y \ln \left(\frac{\xi^2 + r^2}{R^2} \right) \right]. \quad (36)$$

Although Tate [11] used the same expression (35) he apparently did not recognize the result (36), which allows the equation of motion (31) to be integrated exactly pointwise in the entire target region.

The solution in [12] discusses approximate boundary conditions characterizing the free front and rear surfaces of a target of finite thickness. Also, approximate continuity conditions are used at the elastic–plastic boundary which intersects the $r = 0$ axis at the point $z = z_2(t)$, as shown in Fig. 1. For the special case of deep penetration of a long projectile into a semi-infinite target, the effects of the target’s front and rear surfaces and the development of the plastic region can be neglected. In particular, the asymptotic expressions for the contact pressure P applied by the target to the projectile’s surface and for the drag force Σ recorded in [8] yield the normalized results that

$$P(x_s) = Y[P_Y(x_s) + P_I(x_s)\alpha_s], \quad (37a)$$

$$\Sigma(x_s) = \Sigma_Y(x_s) + \Sigma_I(x_s)\alpha_s, \quad (37b)$$

where the functions $\{P_Y, P_I, \Sigma_Y, \Sigma_I\}$ are specified by

$$P_Y(x_s) = \ln \left[\frac{3G}{Y} (1 - x_s^2) \right] + \frac{1}{3} \left(\frac{8 - 9x_s^2}{4 - 3x_s^2} \right),$$

$$P_I(x_s) = \frac{1}{2} (1 - 3x_s^2) (1 - x_s^2),$$

$$\Sigma_Y(x_s) = x_s^2 \ln \left(\frac{3G}{Y} \frac{1}{x_s^2} \right) - (1 - x_s^2) \ln (1 - x_s^2)$$

$$+ \frac{4}{9} \ln \left(\frac{4 - 3x_s^2}{4} \right), \quad \Sigma_I(x_s) = \frac{1}{2} x_s^2 (1 - x_s^2)^2. \quad (38)$$

The value of α_s is determined by the cavitation condition that the pressure $P(x_s)$ vanishes at the cavitation point

$$\alpha_s = \alpha_s(x_s) = -\frac{P_Y(x_s)}{P_I(x_s)} \quad \text{for } \frac{1}{\sqrt{3}} < x_s < 1, \quad (39)$$

where the range of x_s is restricted so that α_s is positive.

Moreover, at the onset of cavitation near the projectile’s nose α_s attains a local minimum value α_c . This occurs for the value of x which satisfies the equation

$$\frac{d\alpha_s(x)}{dx} = \frac{4x}{(1 - 3x^2)^2 (1 - x^2)^2} g_1(x),$$

$$g_1(x) = \frac{-68 + 168x^2 - 189x^4 + 81x^6}{3(4 - 3x^2)^2}$$

$$- 2(2 - 3x^2) \ln \left[\frac{3G(1 - x^2)}{Y} \right]$$

$$= 0 \quad \text{with } \frac{1}{\sqrt{3}} < x < 1. \quad (40)$$

The function $g_1(x)$ has one local maximum in the range of interest. For G/Y smaller than a critical value γ_c the local maximum of $g_1(x)$ is negative and there is no real solution x of Eq. (40). The critical value γ_c of G/Y for the existence of a real solution of x can be determined by solving Eq. (40) for G/Y and writing the solution in the form

$$\frac{G}{Y} = g_2(x),$$

$$g_2(x) = \frac{1}{3(1 - x^2)} \exp \left[\frac{(-68 + 168x^2 - 189x^4 + 81x^6)}{6(4 - 3x^2)^2 (2 - 3x^2)} \right]. \quad (41)$$

It can be shown that the critical value γ_c defined by the minimum value of $g_2(x)$ is obtained when x satisfies the equation

$$g_3(x) = 416 - 1404x^2 + 1716x^4 - 891x^6 + 162x^8 = 0, \quad \sqrt{\frac{2}{3}} < x < 1. \quad (42)$$

The solution of this equation yields the condition that

$$\frac{G}{Y} \geq \gamma_c = 12.4715. \quad (43)$$

If the value of G/Y is greater than γ_c then the local maximum of $g_1(x)$ is positive, which yields two real solutions of Eq. (40). These two solutions are shown in Fig. 3, which plots α_s in Eq. (39) as a function of x_s for $G/Y > \gamma_c$. The smaller solution of Eq. (40), denoted by x_c , causes the function α_s to have a local minimum and it can be used in Eq. (39) to obtain the value α_c of α at the onset of cavitation

$$\alpha_c = \alpha_s(x_c). \quad (44)$$

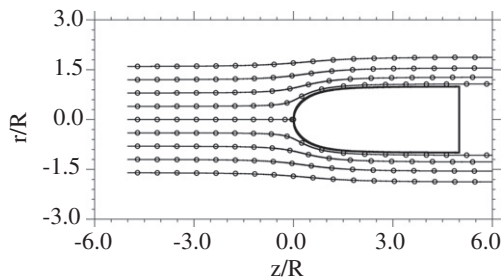


Fig. 2. Streamlines relative to a moving projectile with a nose shape of an ovoid of Rankine. The circles on a given streamline denote the positions of a material point that starts at the left edge and moves towards the right with the time interval between neighboring circles being constant.

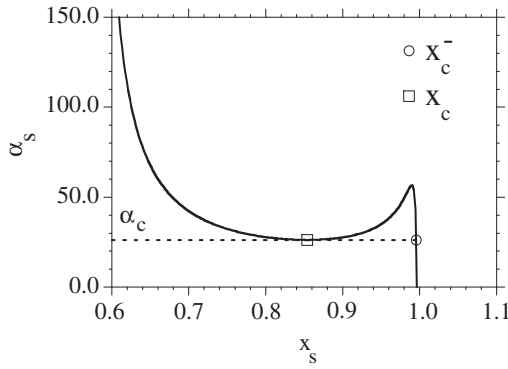


Fig. 3. Plot of α_s (associated with the separation velocity) versus x_s (associated with the normalized separation radius) showing the jump from the tail region x_c^- to the point x_c near the projectile's tip at the value α_c (associated with the minimum cavitation velocity).

Again, for G/Y greater than γ_c there are two solutions of the equation

$$\alpha(x_s) = \alpha_c. \tag{45}$$

The smallest solution is x_c and the largest solution is denoted by x_c^- . For values of penetration velocity V below the cavitation value V_c ($\alpha < \alpha_c$) the separation point x_s remains very close to the projectile's tail ($x_s \approx 1, r \approx R$) which is the branch of the curve in Fig. 3 below the value α_c . When α reaches the cavitation value α_c the separation point jumps from the value x_c^- to x_c , as shown in Fig. 3.

In general, the value of Σ_s in Eq. (38) can be discontinuous at this value of α_c with

$$\Sigma_s(x_c) \neq \Sigma_s(x_c^-). \tag{46}$$

Therefore, the function Σ_s has one branch for $0 \leq \alpha_s \leq \alpha_c$ and another branch for $\alpha_s > \alpha_c$. The separation point x_0 associated with $\alpha_s = 0$ is obtained by using the functional form (39) and solving the equation

$$\alpha_s(x_0) = 0. \tag{47}$$

Then, the complete solution for the drag force Σ can be obtained by evaluating the function (37b) for $x_c^- \leq x_s \leq x_0$ characterizing the lower branch and for $1/\sqrt{3} < x_s \leq x_c$ characterizing the upper branch.

It will be shown that the function (37b) for Σ can be approximated by the simple solution (25) where Σ_c and α_c are given by

$$\Sigma_c = \Sigma(x_c), \quad \alpha_c = \alpha_s(x_c). \tag{48}$$

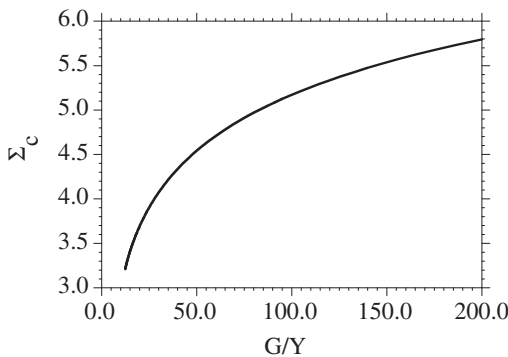


Fig. 4. Plot of $\Sigma_c(x)$ in Eq. (37b) as a function of G/Y in the target using Eq. (41) with $1/\sqrt{3} < x \leq x_c$.

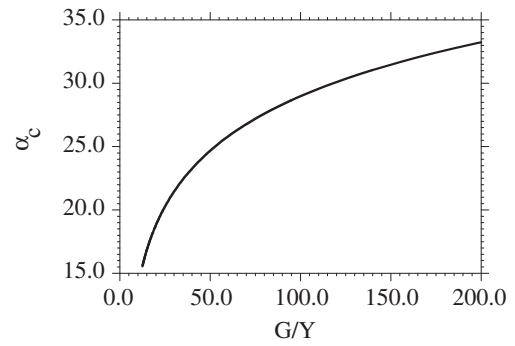


Fig. 5. Plot of $\alpha_c = \alpha_s(x)$ in Eq. (39) as a function of G/Y in the target using Eq. (41) with $1/\sqrt{3} < x \leq x_c$.

in terms of the functions (38) and (39) and the solution x_c of Eq. (40) with the restriction (43). Next, an estimate of the value of β can be obtained by observing from Eqs. (38) and (39) that the value α_s approaches infinity as x_s approaches the value $1/\sqrt{3}$. In this limit resistance of inertia in the target dominates the resistance of plasticity in the target and β attains the limiting value

$$\beta = \beta_\infty = \frac{2}{27} = 0.074074. \tag{49}$$

However, it will be shown that a better approximation of β for lower values of penetration velocity can be obtained by matching the simple solution (25) to the value determined by Eq. (37b) for the maximum value α_{\max} of α in the range of velocities being considered. In particular, using this idea the value x_{\max} is determined by using the functional form (39) and solving the equation

$$\alpha_s(x_{\max}) = \alpha_{\max} \quad \text{with} \quad \frac{1}{\sqrt{3}} < x_{\max} < x_c \quad \text{and} \quad \alpha_{\max} > \alpha_c. \tag{50}$$

Then, the value β_{\max} of β is determined by the expression

$$\beta = \beta_{\max} \left(\frac{G}{Y}, \alpha_{\max} \right) = \frac{\Sigma(x_{\max}) - \Sigma_c}{\alpha_{\max} - \alpha_c}. \tag{51}$$

For the remainder of this paper the value α_{\max} is specified by

$$\alpha_{\max} = 10\alpha_c. \tag{52}$$

With this specification the parameters (27) can be plotted graphically in terms of the value of G/Y . Specifically, Figs. 4–6 show plots of $\Sigma_c(x)$ in (37b), $\alpha_c = \alpha_s(x)$ in Eq. (39) and β_{\max} in Eq. (51) as functions of G/Y using Eq. (41) with $1/\sqrt{3} < x \leq x_c$. Thus, given a value of G/Y for the target these figures can be used to determine

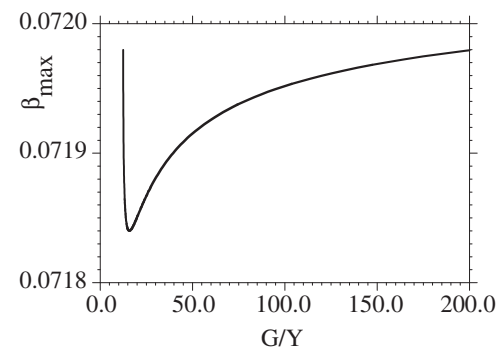


Fig. 6. Plot of β_{\max} in Eq. (51) as a function of G/Y in the target using Eq. (41) with $1/\sqrt{3} < x \leq x_c$ and α_{\max} in Eq. (52).

Table 1
Material parameters and results of the simple formulas.

	Aluminum	Steel
ρ [Mg/m ³]	2.785	7.9
G [GPa]	25.9	76.9
Y [GPa]	0.4	0.4
G/Y	64.75	192.25
Σ_c	4.778	5.761
α_c	26.29	32.99
β_{\max}	0.07193	0.07198
Σ_{cRD}	4.828	5.683
α_{cRD}	32.18	37.88
β_{RD}	0.075	0.075

the values of $\{\Sigma_c, \alpha_c, \beta_{\max}\}$ in the simple form (25) for Σ . Moreover, it can be seen that β_{\max} shown in Fig. 5 is nearly constant and is slightly smaller than the limiting value (49).

3. Examples

In order to examine the validity of the equations developed in Section 2 comparison is made with the results of Rosenberg and Dekel [9] for aluminum and steel targets. Table 1 records the values of the density ρ , shear modulus G , yield strength Y for these materials as well as the values of $\{\Sigma_c, \alpha_c, \beta_{\max}\}$ predicted by the model of Section 2. As mentioned previously the formulas proposed by Rosenberg and Dekel [9] are based on two empirical constants that are obtained by analysis of numerical simulations.

Their formulas were shown to be accurate for two target materials and four nose shapes. In particular, the value β_{RD} in Eq. (21) for an ogival shaped nose was given by

$$\beta_{\text{RD}} = 0.075, \quad (53)$$

which is very close to the value of β_{\max} in Table 1 for the ovoid of Rankine used here. Therefore, for the examples in this section comparison will only be made with the results in [9] for the simulations of an ogive. Table 1 also includes the values of $\{\Sigma_{\text{cRD}}, \alpha_{\text{cRD}}, \beta_{\text{RD}}\}$ obtained using the empirical constants in [9] and the expressions (21). From Table 1 it can be seen that the values of $\{\Sigma_c, \beta_{\max}\}$ obtained analytically are close to the values $\{\Sigma_{\text{cRD}}, \beta_{\text{RD}}\}$ obtained empirically. But the analytical values of α_c are smaller than the empirical values α_{cRD} .

Figs. 7 and 8 show the results for Aluminum and steel, respectively. Specifically, the values of Σ_s are determined by equations (37)–(39) with $x_0 \leq x_s \leq x_c$ for the nearly constant values of Σ_s and with $x_c \leq x_s \leq x_{\max}$ for the higher values of Σ_s . The values of Σ_{simple} and λ_f were determined by Eqs. (25) and (26), respectively, for $0 \leq \alpha \leq \alpha_{\max}$, using the values of $\{\Sigma_c, \alpha_c, \beta_{\max}\}$ reported in Table 1. Similarly, the solution denoted by RD is determined by the expressions (21) and (23) using the values of $\{\Sigma_{\text{cRD}}, \alpha_{\text{cRD}}, \beta_{\text{RD}}\}$ reported in Table 1. These results indicate that the assumption used by Rosenberg and Dekel [9] to reduce the number empirical constants to two has an influence on the value of the velocity (associated with α_c and α_{cRD}) at the onset of cavitation. However, this parameter seems to have a small effect on the predictions of the penetration depth.

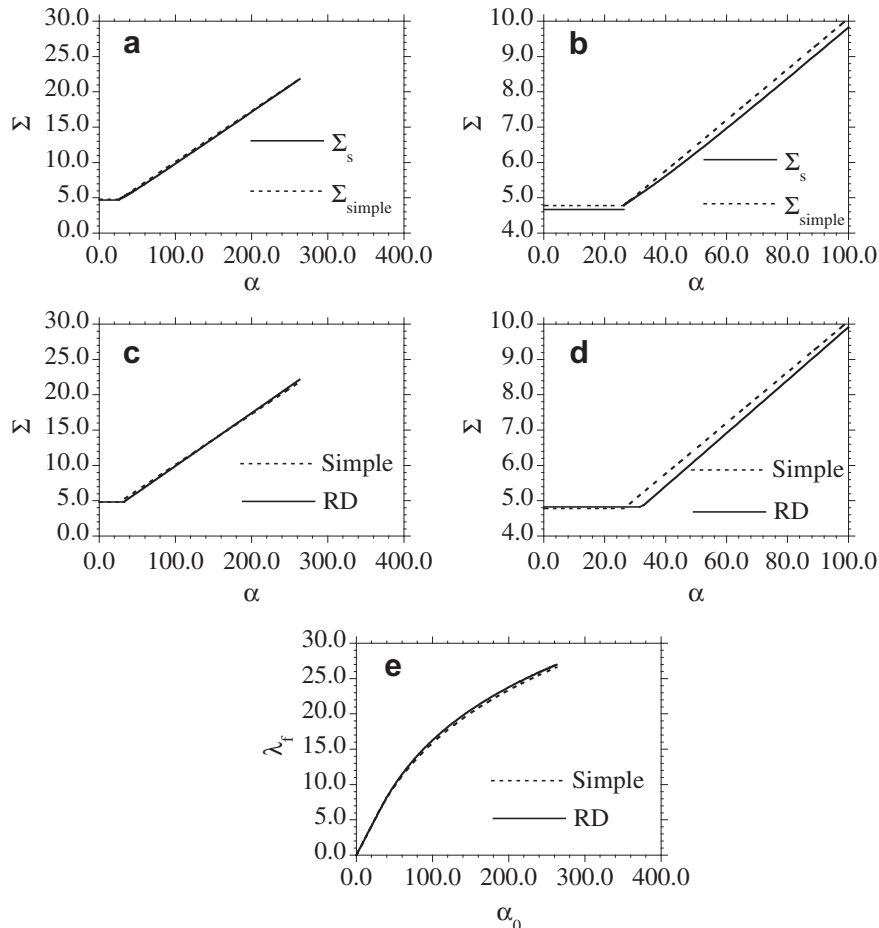


Fig. 7. Aluminum: comparison with the results of Rosenberg and Dekel [9].

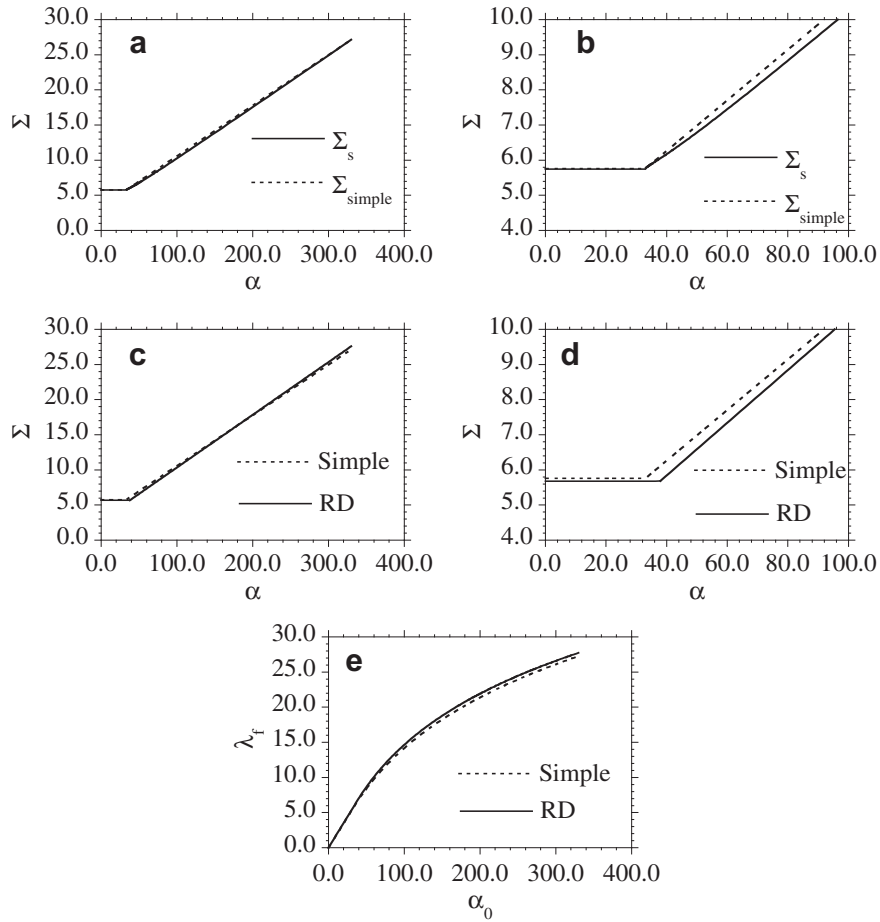


Fig. 8. Steel: Comparison with the results of Rosenberg and Dekel [9].

4. Conclusions and discussion

Yarin et al. [12] developed an analytical solution for penetration of a rigid projectile with a nose shape of an ovoid of Rankine into an incompressible elastic–perfectly-plastic target. Rapoport and Rubin [8] used these analytical expressions to develop simplified equations which predict the drag force and velocity at the onset of cavitation for the full range of impact velocities. Here, these formulas have been used to propose a simplified form Σ_{simple} in Eq. (25) for the drag force applied by the target on the projectile for any penetration velocity. This form depends on three parameters $\{\Sigma_c, \alpha_c, \beta_{\text{max}}\}$ which have been determined analytically in terms of the material constants of the target. Specifically, Σ_c characterizes the constant drag force for penetration velocities V below the value V_c

(associated with α_c) at the onset of cavitation (i.e. separation of the target material from the projectile’s surface) and β_{max} controls the dependence of drag force on inertia in the target for larger values of penetration velocity. This simple form for the drag force is used to obtain an analytical expression for the penetration depth λ_f (26) of a projectile with impact velocity V_0 (associated with α_0). The analytical expressions (25) and (26) for the proposed simplified analytical solution are identical to the empirical expressions (21) and (23) developed by Rosenberg and Dekel [9], except that the empirical expressions depend on only two empirical constants $\{\Sigma_{\text{cRD}}, \beta_{\text{RD}}\}$.

Figs. 7 and 8 suggest that accurate values for the constants $\{\Sigma_c, \alpha_c, \beta_{\text{max}}\}$ can be obtained by plotting the drag force Σ versus α and matching the bilinear form with the expression (25). However,

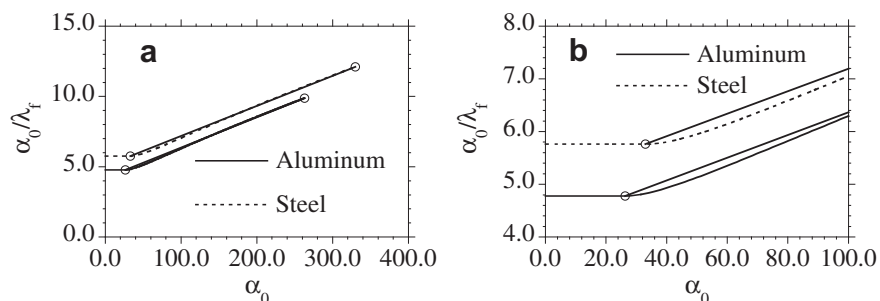


Fig. 9. Plots showing how experimental data for penetration depth might be used to determine the parameters $\{\Sigma_s, \alpha_c, \beta_{\text{max}}\}$ in the simple expression (26).

measurement of the drag force for a range of penetration velocities V is not easy. Instead, most experimental data gives values for the penetration depth λ_f as a function of the impact velocity (associated with α_0). Here, a method is proposed to determine the constants $\{\Sigma_c, \alpha_c, \beta_{\max}\}$ directly from the experimental data for λ_f as a function of α_0 . Specifically, the analytical expression (26) with the constant for Aluminum and Steel in Table 1 is used to generate the plots of α_0/λ_f versus α_0 shown in Fig. 9a,b. Also, included in Fig. 9 are lines connecting the points $\{\alpha_c, \Sigma_c\}$ and $\{\alpha_{\max}, \Sigma_{\text{simple}}(\alpha_{\max})\}$ used to generate these curves. Using the expression Σ_{simple} in Eq. (25) it is clear that the constant value of α_0/λ_f for small values of α_0 determines the constant Σ_c . Moreover, the value of α_c can be estimated by finding the intersection of a straight line that is tangent to the curve for high values of α_0 with the horizontal portion of the curve. Then, the value of β_{\max} can be determined by numerically solving the analytical expression (26) for β_{\max} with $\{\alpha_0, \lambda_f\}$ taken to be the largest values in the data set.

The work in Rosenberg and Dekel [9] shows that their empirical expressions are accurate for a range of nose shapes. In particular, the expressions (21) suggest that Σ_{cRD} and β_{RD} are sensitive to the changes in the nose shape. Since these expressions depend on only two empirical constants it is not clear whether or not the value of α_{cRD} is also sensitive to changes in the nose shape. Consequently, it is not known if the analytical expressions developed here for an ovoid of Rankine can be generalized for different nose shapes or if they can be modified to include the effects of hardening in the target and inevitable deformation of the projectile at high impact velocities.

The work presented here considers penetration of rigid projectiles into incompressible elastic–perfectly plastic targets. The theoretical results have been presented for a large range of impact velocities which include velocities well in excess of the critical value when cavitation occurs and the target material separates from the projectile’s surface at a point on the projectile’s nose. Obviously, projectiles made from real materials will deform and erode above critical values of impact velocities. For example, the work in [7] considered penetration into 6061-T6511 aluminum targets of ogive nosed projectiles made of two steels VAR 4340 and

AerMet 100. It was stated in [7] that as the impact velocity increases: “(1) the projectiles remained rigid and visibly undeformed; (2) the projectile’s deformed during penetration without nose erosion, deviated from the target centerline, and exited the side of the target or turned severely within the target; and (3) the projectile’s eroded during penetration and lost mass.”

Since the projectile’s used in the experiments in [7] had ogive noses it is expected that the predictions of the ovoid of Rankine model (denoted by OR) discussed here should provide reasonably accurate results in comparison with the experimental data. For the following analysis the density ρ of the 6061-T6511 aluminum targets is taken from [7] and the shear modulus G is taken from Table 1 here

$$\rho = 2.710 \text{ Mg/m}^3, \quad G = 25.9 \text{ GPa}. \quad (54)$$

Next, using the value of yield strength $Y = 0.276 \text{ GPa}$ of 6061-T6511 aluminum reported in [7] it is possible to interpolate the results of the OR model given in Figs. 4 and 5 to obtain the theoretical predictions

$$\Sigma_c = 5.1136, \quad \alpha_c = 28.585 \quad (V_c = 1.706 \text{ km/s}) \quad \text{for} \\ Y = 0.276 \text{ GPa}. \quad (55)$$

The radius of each projectile in [7] was $R = 3.555 \text{ mm}$ and the values of the mass of each projectile, the impact velocity and penetration depth are taken from Tables 1 and 2 in [7] for the lower velocities for which the projectiles remained rigid and penetration was rather straight. This data is plotted in Fig. 10. Also, included in Fig. 10 are the theoretical predictions of the OR model using the assumption that the impact velocities are lower than the critical velocity V_c (or α_c) for cavitation to occur. Specifically, for $\alpha_0 \leq \alpha_c$ Eq. (26) yields the theoretical result that

$$\lambda_f = \frac{1}{\Sigma_c} \alpha_0, \quad (56)$$

which is used to plot the straight lines in Fig. 10a,c.

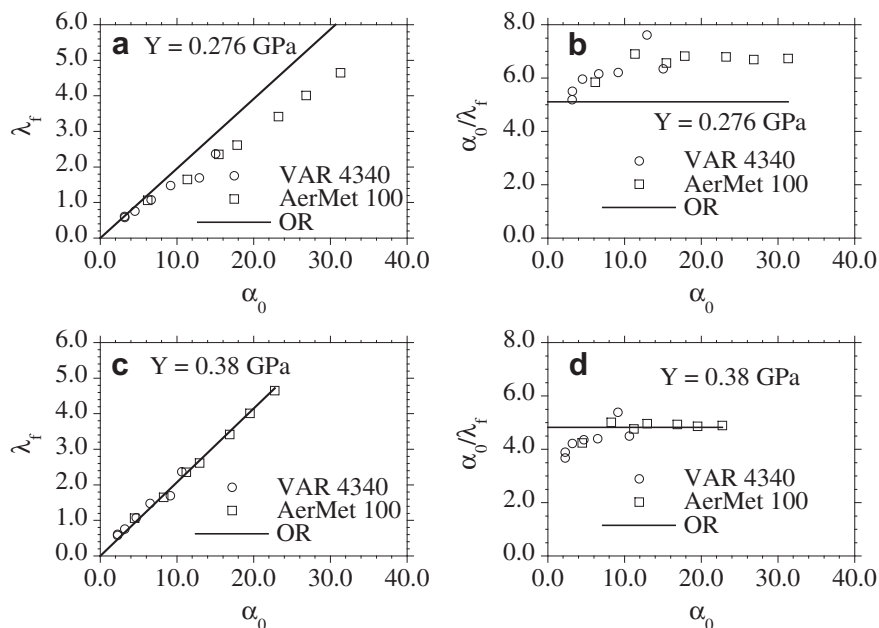


Fig. 10. Analysis of the experimental data in [7] for penetration into targets of 6061-T6511 Aluminum with ogive nosed projectiles made with two steels VAR 4340 and AerMet 100. The solid lines correspond to predictions of ovoid of Rankine model (OR).

The results in Fig. 10a,b indicate that the OR model is inconsistent with the experimental data when $Y = 0.276$ GPa. Moreover, the highest value of α_0 in these figures is greater than the theoretical prediction (55) of the critical value α_c for cavitation. However, using the results in Figs. 4 and 5 it is possible to determine a value for Y which causes the theoretical line (56) to pass through the experimental data point with the highest impact velocity to obtain the theoretical results

$$\Sigma_c = 4.8243, \quad \alpha_c = 26.607 \quad (V_c = 1.9315 \text{ km/s}) \quad \text{for} \\ Y = 0.38 \text{ GPa.} \quad (57)$$

This value of Y is close to the value $Y = 0.4$ GPa listed in Table 1. Moreover, the theoretical results plotted in Fig. 10c are very close to the experimental data and the value of Σ_c in Eq. (57) is within the experimental scatter shown in Fig. 10d. The fact that the experimental data shown in Fig. 10c is well represented by the straight line (56), suggested by the OR model, is a strong indication that the drag force applied by the target on the projectile in this range of velocities is truly constant and is not dependent on the penetration velocity, as suggested by the cavity expansion model. These results are also consistent with the fact that the highest value of α_0 for the experimental data in Fig. 10c,d is less than the theoretical value α_c in Eq. (57) for the onset of cavitation. Apparently, the value of the yield strength Y used in the cavity expansion model must be reduced to compensate for the unphysical dependence of the drag force on penetration velocity in order to approximate experimental data for penetration depth caused by impact velocities below the critical value for cavitation.

Acknowledgements

This research was partially supported by M.B. Rubin's Gerard Swope Chair in Mechanics and by the fund for the promotion of research at the Technion. The author would also like to acknowledge helpful discussions with Z. Rosenberg and E. Dekel.

References

- [1] Alekseevskii VP. Penetration of a rod into a target at high velocity. *Combust Explo Shock Waves* 1966;2:63–6.
- [2] Anderson Jr CE, Morris BL, Littlefield DL. A penetration mechanics database. Southwest Research Institute Report 3593/001; 1992.
- [3] Backman ME, Goldsmith W. The mechanics of penetration of projectiles into targets. *Int J Engng Sci* 1978;16:1–99.
- [4] Batra RC, Wright TW. Steady state penetration of rigid perfectly plastic targets. *Int J Engng Sci* 1986;1986(24):41–54.
- [5] Bishop RF, Hill R, Mott NF. The theory of indentation and hardness tests. *Proc Phys Soc* 1945;57:147–59.
- [6] Hill R. Cavitation and the influence of headshape in attack of thick targets by non-deforming projectiles. *J Mech Phys Solids* 1980;28:249–63.
- [7] Piektyowski AJ, Forrestal MJ, Poormon KL, Warren TL. Penetration of 6061-T6511 aluminum targets by ogive-nose steel projectiles with striking velocities between 0.5 and 3.0 km/s. *Int J Impact Engng* 1999;23:723–34.
- [8] Rapoport L, Rubin MB. Separation and velocity dependence of the drag force applied to a rigid ovoid of Rankine nosed projectile penetrating an elastic–perfectly-plastic target. *Int J Impact Engng* 2009;36:1012–8.
- [9] Rosenberg Z, Dekel E. The penetration of rigid long rods – revisited. *Int J Impact Engng* 2009;36:551–64.
- [10] Tate A. A simple hydrodynamic model for the strain field produced in a target by the penetration of a high speed long rod projectile. *Int J Engng Sci* 1978;16:845–58.
- [11] Tate A. Long rod penetration models – Part I. A flow filed model for high speed long rod penetration. *Int J Mech Sci* 1986;28:535–48.
- [12] Yarin AL, Rubin MB, Roisman IV. Penetration of a rigid projectile into an elastic–plastic target of finite thickness. *Int J Impact Engng* 1995;16:801–31.